

The Impact of Nitrogen Doping on Structural and Electronic Properties of Titanium Sesquioxide, Ti_2O_3 : An *ab-initio* Study

Lynet Allan,^{1,*} George O Amolo,^{2,†} Julius Mwabora,¹ and Silas Mureramanzi¹

¹*Department of Physics, School of Physical Sciences,
University of Nairobi, P.O.Box 30197-00100 Nairobi Kenya.*

²*Materials Modeling Group, School of Physics and Earth Sciences,
The Technical University of Kenya, 52428-00200, Nairobi, Kenya.*

(Dated: January 4, 2022)

Titanium based oxides are abundant, chemically stable, non-toxic, and highly versatile materials, with applications ranging from photovoltaics to catalysis. For rutile and anatase phases of TiO_2 , the bandgap ranges from 3.0–3.2 eV, which are too large to absorb in the visible range (400 nm - 700 nm), resulting in poor photo-catalytic efficiency. Nitrogen doping into TiO_2 has been able to narrow its bandgap, forming an absorption tail in the visible-light region. However, TiO_2 has limits to which it can be doped, suggesting investigations of the oxygen-deficient Ti_2O_3 . Using the state-of-the-art Density Functional Theory (DFT) as implemented in the Quantum ESPRESSO package, we report on the structural and electronic properties of corundum-type $\text{Ti}_2\text{N}_2\text{O}$ (an example $\text{Ti}_n\text{N}_2\text{O}_{2n-3}$ compound with $n=2$). The most stable sample of the oxynitride ($\text{Ti}_2\text{N}_2\text{O}$ -P1), has a bandgap of 2.2 eV, which is clearly near the middle of visible light, and has no in-gap states, suggesting that they are more efficient visible-light-driven materials for photocatalytic applications compared to TiO_2 , TiO_2 : N and Ti_2O_3 .

Key words: DFT, Ti_2O_3 , $\text{Ti}_2\text{N}_2\text{O}$, structural and electronic properties.

I. INTRODUCTION

Due to increasing global energy demands and the harmful environmental pollution caused by the combustion of fossil fuels, the quest for sustainable alternative energy resources has become a major area of research¹. Ti-based oxides have been intensively investigated as photo-catalysts due to their wide applications in environmental remediation and solar energy conversion^{2,3}. Despite having wide bandgaps of 3.0 eV and 3.2 eV, respectively, rutile and anatase phases of titanium dioxide (TiO_2) still attracts considerable attention³⁻¹⁰. To improve the solar application efficiency of Ti-based oxides, there has been an attempt to narrow their bandgap to absorb a major part of the solar spectrum¹¹. Doping is considered to be one of the promising methods of narrowing the bandgap of the Ti-based oxides¹². Previous *ab-initio* works have been reported on doped TiO_2 compounds. V, Cr, Mn, Fe, and Ni have been doped into TiO_2 at the Ti sites^{13,14}, such cationic doping leads to the localized d-states deep in the bandgap of TiO_2 , which would act as the recombination centers for photoexcited electrons and holes, lowering photocatalytic activity. An anion doping in TiO_2 with N, C, S, and B has been equally explored¹⁵⁻¹⁸, such resulted in the p-states near the valence band being similar to other deep donor levels in the semiconductor¹⁸. Owing to the finite number of oxygen vacancies, TiO_2 has limits to which it can be doped¹⁹. In this work, we increase nitrogen concentrations in titanium oxide systems by considering compounds having the composition $\text{Ti}_n\text{O}_{2n-1}$, rather than TiO_2 with a finite number of oxygen vacancies. These systems can be viewed as ordered oxygen-deficient TiO_2 variants with a lot of oxygen vacancies which allows nitrogen substitutions, hence,

should be able to accommodate far greater nitrogen concentrations than TiO_2 . In search of novel photocatalytic materials that are stable, efficient, and capable of being visible light driven, Wu and his co-workers⁹, using high throughput screening method within density functional theory (DFT)²⁰, discovered $\text{Ti}_n\text{N}_2\text{O}_{2n-3}$ compound for the $n=3$ case ($\text{Ti}_3\text{N}_2\text{O}_3$), which they predicted to be synthesizable, suitable for visible light (or UV light) absorption, and energetically favorable to catalyze the water-splitting reaction.

Corundum Ti_2O_3 , a Ti based oxide with nominal $\text{Ti}_n\text{O}_{2n-1}$, $n=2$ configuration together with its oxynitrides $\text{Ti}_n\text{N}_2\text{O}_{2n-3}$, $n=2$, ($\text{Ti}_2\text{N}_2\text{O}$), has been much less investigated. Here, we explore the structural and electronic properties of Corundum Ti_2O_3 using Density Functional Theory (DFT) and Density Functional Theory with the inclusion of Hubbard U correction (DFT+ U)²¹ studies. In particular, we employ nitrogen substitutional doping at oxygen sites. The structural and electronic properties of the pristine and doped oxides, with and without the inclusion of Hubbard U , are simulated and analyzed. This study provides complementary theoretical data on structural and electronic properties of anionic doping of Ti_2O_3 with nitrogen.

II. COMPUTATIONAL DETAILS

We have carried out simulations on trigonal Ti_2O_3 with $a = b = c$, $\alpha = \beta = \gamma \neq 90^\circ$ within density functional theory (DFT)²⁰ using the generalized gradient approximation (GGA) as implemented in the Quantum ESPRESSO(QE) code²². The electron-ion interactions are described by ultra-soft pseudo-potentials²³

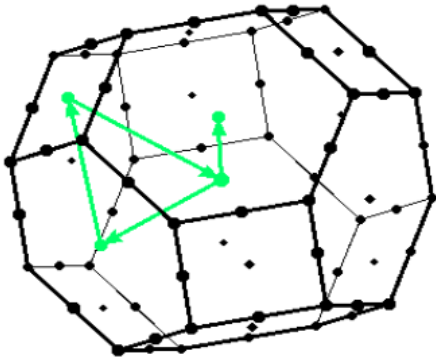


FIG. 1. Brillouin zone integration for Corundum Ti_2O_3 showing the origin at Γ

drawn from the 2.0.1 version of the library of Dal Corso et al,(2001)⁶. For the exchange-correlation interaction, the enhanced Perdew-Burke- Ernzerhof functional of the generalized gradient approximation, for solids (GGA-PBESol)²⁴ are employed. This exchange-correlation is selected because it is computationally efficient and no adjustable parameter is required. An extra Hubbard U term is included to account for the strong electron correlations, with U values tested in the range of 1 eV - 7 eV, applied only to the Ti-3d orbitals in Ti_2O_3 . The wave functions for valence electrons are expanded through a plane-wave basis set within the energy cut-off of 30 Ry. The atomic coordinates are relaxed until the forces are less than 0.01 eV/Å. The crystal structures are then viewed using the X-window Crystalline and Molecular Structure Visualization (XCrysDen)²⁵ program where the lattice parameters a and c for the pristine and doped structures with and without the inclusion of the hubbard U , are determined. A Monkhorst-Pack mesh sampling²⁶ equivalent to $5 \times 5 \times 5$ are employed. For band structure calculations, explicit positions along the high symmetry axes are described on the path $\Gamma \rightarrow Z \rightarrow F \rightarrow \Gamma \rightarrow L$ ²⁷ shown in Fig 1.

III. RESULTS AND DISCUSSIONS

A. Structural Properties: Lattice Parameters

By fitting the energy volume relationship to the Mur-naghan equation of state²⁸, the volume that yields the minimum energy value are obtained. From table I the calculated lattice parameters a and c (at $U=0$ eV) lie slightly above the experimental data²⁹. It is well known that GGA tends to overestimate the lattice parameters³⁰. The slight deviations are attributed to the fact that simulations have not taken into account the existence of intrinsic and other defects occurring in actual situations. To check on the feasibility of the doped systems, the structural properties of pure and doped Ti_2O_3 are compared. After the doping process, the lattice constants of

doped systems are found to be slightly deformed, showing lattice strain due to the difference in radius between the dopant N atom(s) and the substituted O atom(s). The optimized lattice parameters for undoped Ti_2O_3 are $a=b=c$ 5.274 Å, while for doped systems are $a=b=c$ 5.271 Å. This result is consistent with the experimental results²⁹, as well as other theoretical studies⁴, demonstrating the accuracy and dependability of the structural optimization parameters and method used.

To account for the strong electron correlations, an extra Hubbard- U term is added, with a U_{eff} of 1 eV - 7 eV applied only to the Ti-3d orbitals. As seen in Table I, there are some slight changes in the lattice parameter. To be more exact, the c/a ratio is seen to be decreasing with increasing values of U at some point. The inclusion of the U values in this computation is likely to have resulted in changes in the lattice parameters due to the correction of hybridization between O-2p and Ti-3d orbitals³¹. As a result, the ideal value of U is determined by seeking a fair agreement with experimental data for both structural and electronic properties.

TABLE I. Variation of lattice parameters and calculated band gaps with increasing Hubbard U Values for Corundum Ti_2O_3

U Values (eV)	Lattice Parameters a(Å) c/a		Band gaps (eV)
0	5.27	1.03	No gap
1	5.22	1.03	0.11
2	5.24	1.02	0.49
3	5.25	1.02	0.87
4	5.19	1.01	1.36
5	5.16	1.00	1.63
6	5.38	1.00	1.76
7	5.35	1.03	1.86
Expt ²⁹	5.15	1.01	1.65

B. Choice of Hubbard U for Ti_2O_3

Corundum Ti_2O_3 , appeared metallic, as shown in Fig 7(a), this is consistent with other DFT findings⁴. Experimental studies by Li et al (2018)²⁹, however, show that Corundum Ti_2O_3 has a bandgap of 1.65 eV. As expected, Kohn-Sham DFT calculations could not predict this small gap since it is known to underestimate the bandgaps of systems with d and f orbitals³². A moderated Hubbard potential, U , applied to the calculations of electronic structures leads to more precise electronic band gaps. The U values are optimized empirically by tuning the values of U when seeking an agreement with the experimental results of the properties of the Ti_2O_3 ³², as well as checking on the impact on lattice parameters as indicated in Table I. One thing that came out clear was that the value of the energy gap kept increasing in an almost linearly manner with the U values as shown in Fig 2. Corundum Ti_2O_3 opened a 1.638 eV band gap by

DFT+U ($U=5$ eV) studies, supporting the experimental data that this structure has semiconducting properties. The lattice parameter at $U=5$ eV presented in Table I is also in good agreement with the experimental lattice parameter²⁹ of 5.15 eV. The value, $U = 5$ eV, is therefore considered as the optimal value and inferred for improved prediction of the band gap of the corundum based $\text{Ti}_2\text{N}_2\text{O}$ structures.

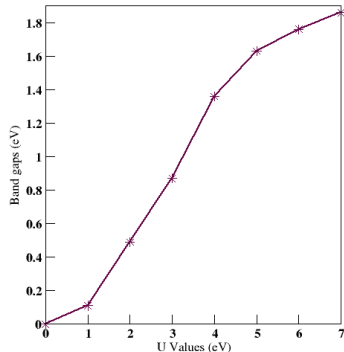


FIG. 2. Variations of band gaps with increasing values of U

C. Nitrogen substituted Ti_2O_3 ($\text{Ti}_2\text{N}_2\text{O}$)

By substituting two of the $2n - 1$ oxygen atoms of $\text{Ti}_n\text{O}_{2n-1}$ compounds with nitrogen, a series of $\text{Ti}_2\text{N}_2\text{O}$ oxynitrides are modelled. Four out of six oxygen atoms are substituted with nitrogen to obtain $\text{Ti}_2\text{N}_2\text{O}$ compounds. Due to the symmetry of the parent material, only three types (P1, P2, and P3) shown in Fig 3 are considered.

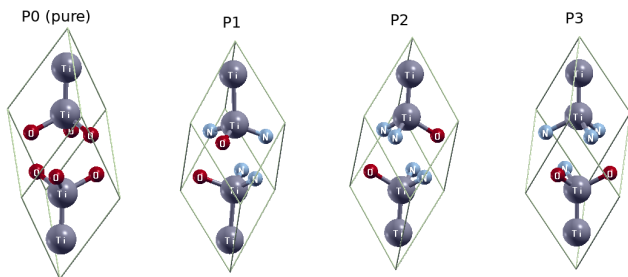


FIG. 3. (Color online) (P0) Pure Corundum Ti_2O_3 [R3c (No. 167), trigonal], (P1)-(P3) Different orientations of Nitrogen substitutions in Ti_2O_3 structure. P2 has an inversion symmetry while P1 and P3 do not have.

The other alternative is to model the oxynitrides in the hexagonal convectional cells of Ti_2O_3 containing 30 atoms (twelve titanium and eight oxygen atoms)⁴. This is as well considered and viewed at three different angles of projection in Fig 4. Twelve out of eighteen oxygen atoms are replaced by nitrogen in seven different ways

to form seven samples of $\text{Ti}_2\text{N}_2\text{O}$ oxynitrides, projected in the a+b direction (for a clearer view), and arranged according to their stability as S1-S7, (S1 being the most stable sample) as shown in Fig 5.

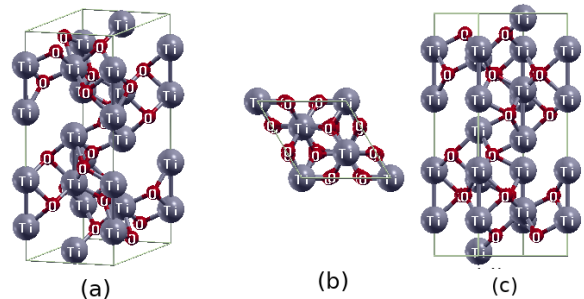


FIG. 4. (Color online) Three different angles of projection of Ti_2O_3 hexagonal convectional cell (a) Bird's eye view (b) Top view, and (c) Projected in the direction of a+b.

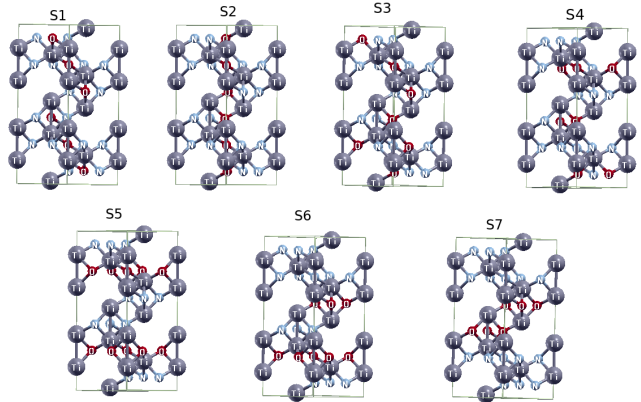


FIG. 5. (Color online) Seven samples of $\text{Ti}_2\text{N}_2\text{O}$ (S-structures)

The stability of $\text{Ti}_2\text{N}_2\text{O}$ (P and S) corundum based structures, are then compared as shown in Fig 6.

P-structures have lower formation energies than S-structures from Fig 6, hence more stable, with P1 being the most stable sample of all. This is well in agreement with the theory of Aoki et al.(2019)⁴, where GW studies were employed to study the structures. Therefore, the P structures are considered for further analysis of the band structures and projected density of state (PDOS) shown in Fig 7.

D. Band structures and Projected Density of States

To explore the effect of doping on the electronic properties of Ti_2O_3 and clarify the origin of improved visible light photo activity, the band structures and projected density of states (PDOS) are calculated as given in Fig

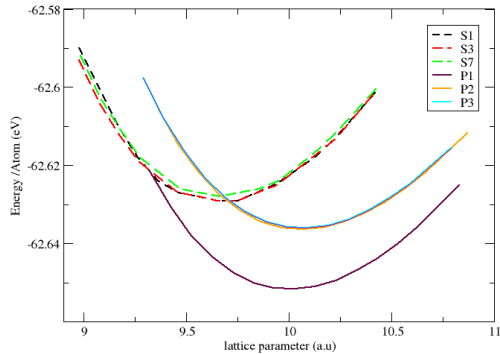


FIG. 6. Plots for energy/cell (eV) against lattice parameter for both S- and P-structures.

7. For ease of comparison, the Fermi level (E_f) is set at zero. With Ti-3d/ O-2p orbitals dominant in the entire band structure, Corundum Ti_2O_3 appeared metallic, as shown in Fig 7(a).

Fig 7(b)-(d) shows that nitrogen substitution into corundum Ti_2O_3 opens up a gap of 2.2 eV by DFT+U studies with $U=5$ eV in the P1 sample (most stable) while the P2 and P3 samples have band gaps of 1.98 eV and 1.92 eV, respectively. The electronic structure of Ti_2O_3 changes as the lattice parameters and deformation around the dopants changes, modifying their photocatalytic activity. In all three (P1, P2 and P3) samples, indirect bandgaps with bandgap character of Ti-3d/N-2p orbitals are observed. Some hybridization between N-2p and Ti-3d states is also observed in the valence band, although there are no in-gap states within the intrinsic gap, as there are in TiO_2 doped nitrogen³¹, thus the absorption threshold is unlikely to be affected. We have obtained a Ti-based oxide with a reduced band gap compared to the highly investigated TiO_2 , without necessarily creating the in-gap states which are known to serve as recombination centers for the photo-excited electrons and holes. This study suggests that, relative to pristine TiO_2 , Ti_2O_3 and $TiO_2:N$ compounds, Ti_2N_2O structures are more promising photo-catalytic/photo-voltaic materials. Table II offers a description of a comparison of the calculated and experimental bandgap for the oxides.

IV. CONCLUSION

Using the DFT and DFT+U approach, we have investigated the effect of nitrogen substitution on the ge-

ometry and electronic structure of corundum Ti_2O_3 in order to enhance its photo-catalytic performance. Significant structure information which may be useful in guiding experimental work as well as identifying appropriate applications for the material has been obtained. Structural and electronic properties of corundum Ti_2O_3 and the oxynitrides Ti_2N_2O have been analysed in this work. With regard to the impact of the Hubbard U parameter on both structural and electronic properties, the best value of U is found to be 5 eV. Even though these calculations assume defect-free structures, the lattice parameters and band gap obtained for this value of U are in good agreement with other DFT results and experimental data. The oxygen deficient corundum Ti_2O_3 , which showed metal-like properties opens up a bandgap of 1.638 eV by DFT+U ($U=5$ eV) studies, agreeing well with reported experimental data. To enhance photo-activity of Ti-based oxides, without creating mid-gap states, we aimed at reducing the band gaps of the oxides. This was achieved in Ti_2N_2O structures, which had a bandgap of 2.2 eV (563.56 nm), in the most stable sample_P1, and had no in-gap states. In principle, Ti_2N_2O materials are found to be better for photo-catalytic/ photo-voltaic applications, compared to TiO_2 , $TiO_2:N$ and Ti_2O_3 materials.

V. ACKNOWLEDGMENTS

This research was supported by the International Science Program (UON 500-661-127, PI- Prof. Aduda Bernard O.), through condensed matter thematic group of the Department of Physics, University of Nairobi. The Centre of High-Performance Computing (CHPC) through the project MATS862, Rosebank Cape Town Republic of South Africa is appreciated for providing access to the HPC cluster facility used in this research. Much appreciation to the Materials Modeling Group at the Technical University of Kenya for support.

VI. CONFLICTS OF INTEREST

There is no conflict of interest.

* lynetamondi3@gmail.com

† georgeamollo862@gmail.com

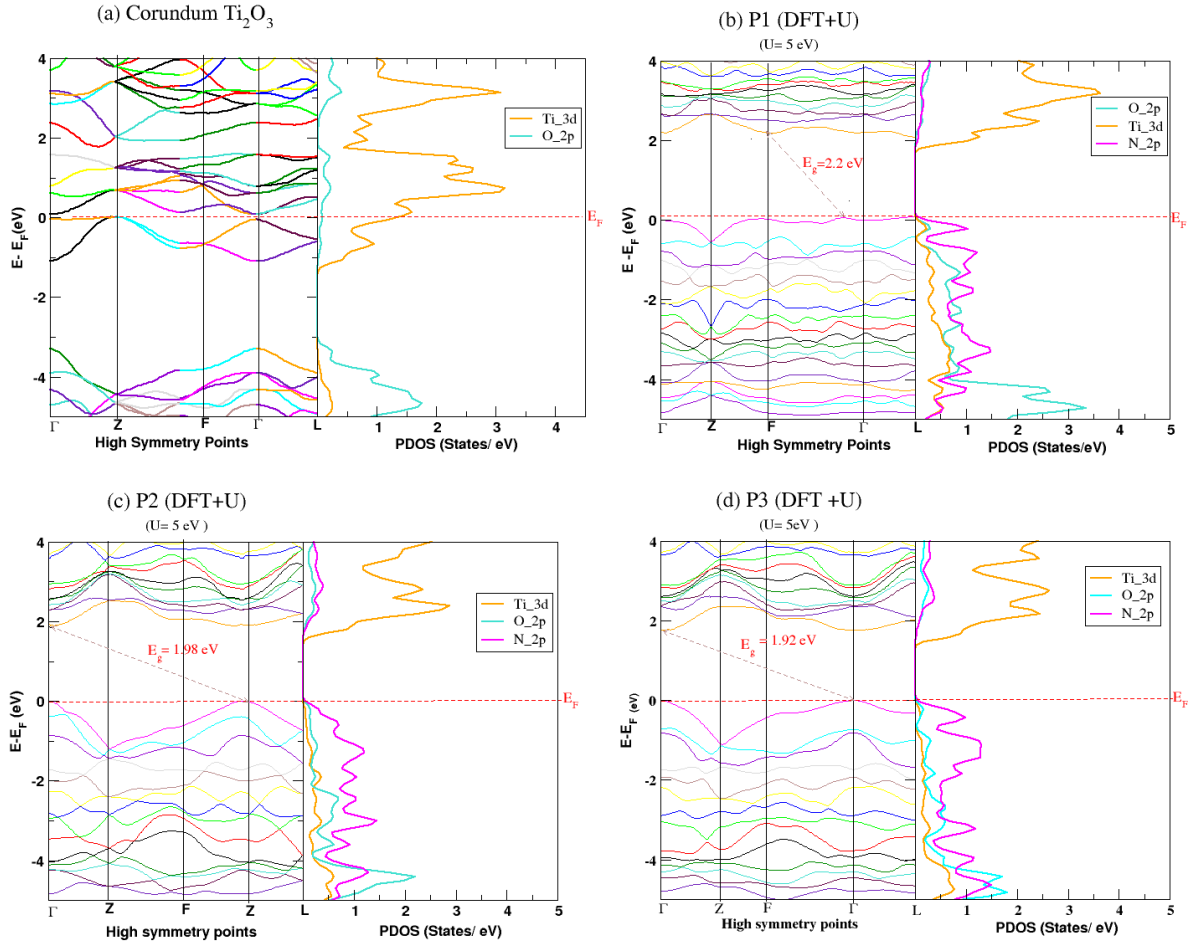


FIG. 7. Band structures and Pdos for Corundum-based $\text{Ti}_2\text{N}_2\text{O.P}$ structures using DFT+U ($U=5$ eV) method.

TABLE II. Summary of the comparison of the calculated and experimental bandgap for the structures

MATERIAL	ENERGY BAND GAP (eV)		
	THIS WORK (GGA)	THEORETICAL (GGA)	THIS WORK EXPERIMENTAL
Corundum Ti_2O_3	No gap	No gap ⁴	1.64($U=5$ eV) 1.65 ²⁹
Oxynitrides			
$\text{Ti}_2\text{N}_2\text{O}$ (P1)			2.20 ($U=5$ eV)
$\text{Ti}_2\text{N}_2\text{O}$ (P2)			1.98 ($U=5$ eV)
$\text{Ti}_2\text{N}_2\text{O}$ (P3)			1.92 ($U=5$ eV)

- ¹ B. Shaffer, *MRS Energy & Sustainability* **6** (2019).
- ² R. Daghrir, P. Drogui, and D. Robert, *Industrial & Engineering Chemistry Research* **52**, 3581 (2013).
- ³ T. E. Agustina, H. M. Ang, and V. K. Vareek, *Journal of Photochemistry and Photobiology C: Photochemistry Reviews* **6**, 264 (2005).
- ⁴ Y. Aoki, M. Sakurai, S. Coh, J. R. Chelikowsky, S. G. Louie, M. L. Cohen, and S. Saito, *Physical Review B* **99**, 075203 (2019).
- ⁵ M. O. Atambo, D. Varsano, A. Ferretti, S. S. Ataei, M. J. Caldas, E. Molinari, and A. Selloni, *Physical Review Materials* **3**, 045401 (2019).
- ⁶ Q. M. Carlo, .
- ⁷ A. Fujishima, T. N. Rao, and D. A. Tryk, *Journal of photochemistry and photobiology C: Photochemistry reviews* **1**, 1 (2000).
- ⁸ Y. Li, *Investigation of Titanium Sesquioxide Ti₂O₃: Synthesis and Physical Properties*, Ph.D. thesis (2016).
- ⁹ Y. Wu, P. Lazic, G. Hautier, K. Persson, and G. Ceder, *Energy & environmental science* **6**, 157 (2013).
- ¹⁰ K. Shirai, G. Fazio, T. Sugimoto, D. Selli, L. Ferraro, K. Watanabe, M. Haruta, B. Ohtani, H. Kurata, C. Di Valentin, *et al.*, *Journal of the American Chemical Society* **140**, 1415 (2018).
- ¹¹ M. Khan, J. Xu, N. Chen, and W. Cao, *Journal of Alloys and Compounds* **513**, 539 (2012).
- ¹² W. Guo, L. Wu, Z. Chen, G. Boschloo, A. Hagfeldt, and T. Ma, *Journal of Photochemistry and Photobiology A: Chemistry* **219**, 180 (2011).
- ¹³ S. N. R. Inturi, T. Boningari, M. Suidan, and P. G. Smirnotis, *Applied Catalysis B: Environmental* **144**, 333 (2014).
- ¹⁴ T. Umebayashi, T. Yamaki, H. Itoh, and K. Asai, *Journal of Physics and Chemistry of Solids* **63**, 1909 (2002).
- ¹⁵ T. Morikawa, R. Asahi, T. Ohwaki, K. Aoki, and Y. Taga, *Japanese Journal of Applied Physics* **40**, L561 (2001).
- ¹⁶ A. Fujishima, X. Zhang, and D. A. Tryk, *Surface science reports* **63**, 515 (2008).
- ¹⁷ S. Sakthivel and H. Kisch, *Angewandte Chemie International Edition* **42**, 4908 (2003).
- ¹⁸ J. Schneider, M. Matsuoka, M. Takeuchi, J. Zhang, Y. Horiuchi, M. Anpo, and D. W. Bahnemann, *Chemical reviews* **114**, 9919 (2014).
- ¹⁹ S. Shevlin and S. Woodley, *The Journal of Physical Chemistry C* **114**, 17333 (2010).
- ²⁰ W. Kohn and L. J. Sham, *Phys. Rev.* **140**, A1133 (1965).
- ²¹ B. Himmetoglu, A. Floris, S. De Gironcoli, and M. Cococcioni, *International Journal of Quantum Chemistry* **114**, 14 (2014).
- ²² P. Giannozzi, S. Baroni, N. Bonini, M. Calandra, R. Car, C. Cavazzoni, D. Ceresoli, G. L. Chiarotti, M. Cococcioni, I. Dabo, A. D. Corso, S. de Gironcoli, S. Fabris, G. Fratesi, R. Gebauer, U. Gerstmann, C. Gougoussis, A. Kokalj, M. Lazzeri, L. Martin-Samos, N. Marzari, F. Mauri, R. Mazzarello, S. Paolini, A. Pasquarello, L. Paulatto, C. Sbraccia, S. Scandolo, G. Sclauzero, A. P. Seitsonen, A. Smogunov, P. Umari, and R. M. Wentzcovitch, *Journal of Physics: Condensed Matter* **21**, 395502 (2009).
- ²³ G. Kresse and D. Joubert, *Phys. Rev. B* **59**, 1758 (1999).
- ²⁴ J. P. Perdew, K. Burke, and M. Ernzerhof, *Phys. Rev. Lett.* **77**, 3865 (1996).
- ²⁵ A. Kokalj and M. Causà, “Xcrysden:(x-window) crystalline structures and densities,” (2001).
- ²⁶ H. J. Monkhorst and J. D. Pack, *Phys. Rev. B* **13**, 5188 (1976).
- ²⁷ W. Setyawan and S. Curtarolo, *Computational materials science* **49**, 299 (2010).
- ²⁸ F. Murnaghan, *Proceedings of the national academy of sciences of the United States of America* **30**, 244 (1944).
- ²⁹ Y. Li, Y. Yang, X. Shu, D. Wan, N. Wei, X. Yu, M. B. Breese, T. Venkatesan, J. M. Xue, Y. Liu, *et al.*, *chemistry of materials* **30**, 4383 (2018).
- ³⁰ M. Niu, W. Xu, X. Shao, and D. Cheng, *Applied Physics Letters* **99**, 203111 (2011).
- ³¹ C. Persson and S. Mirbt, *Brazilian journal of physics* **36**, 286 (2006).
- ³² Z. Hu and H. Metiu, *The Journal of Physical Chemistry C* **115**, 5841 (2011).